October 12, 2015

ATAF2 integrates Arabidopsis brassinosteroid inactivation and seedling photomorphogenesis

Hao Peng
Jianfei Zhao, *University of Pennsylvania*
Michael Neff

© 2015. Published by The Company of Biologists Ltd | Development (2015) 142, 4129-4138 doi:10.1242/dev.124347

RESEARCH ARTICLE

ATAF2 integrates *Arabidopsis* brassinosteroid inactivation and seedling photomorphogenesis

Hao Peng[1], Jianfei Zhao[1,2,*] and Michael M. Neff[1,2,‡]

ABSTRACT

The *Arabidopsis thaliana* hypocotyl is a robust system for studying the interplay of light and plant hormones, such as brassinosteroids (BRs), in the regulation of plant growth and development. Since BRs cannot be transported between plant tissues, their cellular levels must be appropriate for given developmental fates. BR homeostasis is maintained in part by transcriptional feedback regulation loops that control the expression of key metabolic enzymes, including the BR-inactivating enzymes BAS1 (CYP734A1, formerly CYP72B1) and SOB7 (CYP72C1). Here, we find that the NAC transcription factor (TF) ATAF2 binds the promoters of *BAS1* and *SOB7* to suppress their expression. ATAF2 restricts the tissue-specific expression of BAS1 and SOB7 *in planta*. *ATAF2* loss- and gain-of-function seedlings have opposite BR-response phenotypes for hypocotyl elongation. ATAF2 modulates hypocotyl growth in a light-dependent manner, with the photoreceptor phytochrome A playing a major role. The photomorphogenic phenotypes of *ATAF2* loss- and gain-of-function seedlings are suppressed by treatment with the BR biosynthesis inhibitor brassinazole. Moreover, the disruption of *BAS1* and *SOB7* abolishes the short-hypocotyl phenotype of *ATAF2* loss-of-function seedlings in low fluence rate white light, demonstrating an ATAF2-mediated connection between BR catabolism and photomorphogenesis. *ATAF2* expression is suppressed by both BRs and light, which demonstrates the existence of an ATAF2-BAS1/SOB7-BR-ATAF2 feedback regulation loop, as well as a light-ATAF2-BAS1/SOB7-BR-photomorphogenesis pathway. ATAF2 also modulates root growth by regulating BR catabolism. As it is known to regulate plant defense and auxin biosynthesis, ATAF2 therefore acts as a central regulator of plant defense, hormone metabolism and light-mediated seedling development.

KEY WORDS: Seedling development, Hypocotyl growth, Photomorphogenesis, Brassinosteroids, Transcription factor, Cytochrome P450

INTRODUCTION

Multiple hormonal and light signals coordinately regulate plant morphogenesis (Neff et al., 2000; Gray, 2004). The *Arabidopsis thaliana* hypocotyl is a robust system for studying the interplay of light and plant hormones in the regulation of plant growth and development (Collett et al., 2000; Vandenbussche et al., 2005). Genetic screens for long-hypocotyl mutants in the light led to the isolation of genes involved in photomorphogenic signaling pathways, including many of the photoreceptors (Neff and Chory, 1998). Screens for short-hypocotyl mutants in the dark have also identified additional genes involved in photomorphogenesis-regulating pathways, including those associated with hormone-mediated development (Chory et al., 1989). For example, the dark-grown short-hypocotyl mutant *det2* uncovered the role of brassinosteroids (BRs) in seedling growth and development (Chory et al., 1991; Li et al., 1996).

Brassinolide (BL) is the endpoint of the BR biosynthetic pathway in many plant species and confers the strongest biological activity (Yokota, 1997). The BR signaling (Zhu et al., 2013) and metabolism (Zhao and Li, 2012) pathways have been well studied in *Arabidopsis*. Loss-of-function mutations in key BR biosynthesis genes leads to BR deficiency-specific dwarfism of *Arabidopsis* plants, which can be rescued in a dose-dependent manner by exogenous BR (Zhao and Li, 2012). By contrast, a BR-deficient dwarf phenotype is conferred by overexpression (or gain-of-function) of BR catabolic enzymes, such as the cytochrome P450s BAS1 (CYP734A1, formerly CYP72B1) and SOB7 (CYP72C1) (Neff et al., 1999; Turk et al., 2003, 2005; Thornton et al., 2010).

BRs cannot be transported between plant tissues (Savaldi-Goldstein et al., 2007; Symons et al., 2008). Since BRs are synthesized and perceived in the same tissues, homeostasis of this class of hormones is tightly regulated to ensure that their cellular levels are appropriate for a given developmental fate. BR homeostasis is also important for the establishment of plant immunity (Belkhadir et al., 2012).

In *Arabidopsis*, BR homeostasis is maintained in part by transcriptional feedback regulation loops that control the expression of key biosynthetic and catabolic enzymes (Tanaka et al., 2005). For example, TCP1, a putative bHLH transcription factor (TF), interacts with the promoter of the BR biosynthesis gene *DWF4* (Choe et al., 1998) to modulate BR levels (Guo et al., 2010). In addition, the TF LATERAL ORGAN BOUNDARIES (LOB) binds directly to the promoter of *BAS1* as an activator, and consequently reduces BR accumulation to limit growth in organ boundaries (Bell et al., 2012).

In this research, we found that an *Arabidopsis* NAC (NAM, ATAF1,2 and CUC2) family TF, ATAF2 (ANAC081), binds the promoters of *BAS1* and *SOB7* to suppress their expression. ATAF2 regulates hypocotyl elongation and root growth by suppressing BR catabolism. The expression of *ATAF2* is suppressed by both BRs and light. The photomorphogenic phenotypes of *ATAF2* loss- and gain-of-function seedlings can be suppressed by treatment with the BR biosynthesis inhibitor brassinazole (BRZ) (Asami et al., 2000). Moreover, the disruption of *BAS1* and *SOB7* abolishes the short-hypocotyl phenotype of *ATAF2* loss-of-function seedlings in low fluence rate white light, which demonstrates an ATAF2-mediated connection between BR catabolism and photomorphogenesis. We propose that ATAF2 plays a central role in integrating BR homeostasis and seedling development. Considering that ATAF2 has previously

[1]Department of Crop and Soil Sciences, Washington State University, Pullman, WA 99164, USA. [2]Molecular Plant Science Graduate Program, Washington State University, Pullman, WA 99164, USA.
*Present address: Department of Biology, University of Pennsylvania, Philadelphia, PA 19104, USA.

‡Author for correspondence (mmneff@wsu.edu)

Received 13 March 2015; Accepted 12 October 2015

Development (2015) 142, 4129-4138 doi:10.1242/dev.124347

been identified as a regulator of plant defense (Delessert et al., 2005; Wang et al., 2009) and the auxin biosynthesis gene *NIT2* (Huh et al., 2012), ATAF2 acts as a central regulator of plant defense, hormone metabolism and light-mediated seedling development.

RESULTS

ATAF2 binds to the promoters of *BAS1* and *SOB7*

In a yeast one-hybrid (Y1H) screen for the potential protein interactors of the *BAS1* promoter, a truncated ATAF2 missing the first 65 amino acids (ATAF2t) was found to interact with a *BAS1* promoter fragment (−731 to −504) (Table S1). This fragment, p*BAS1*-EE, contains only an Evening Element TF binding site (EE; AAAATATCT or its complementary sequence) (Michael and McClung, 2002) when scanned with the Athena program (O'Connor et al., 2005). Thus, the EE element was proposed to be the ATAF2 binding target in the *BAS1* promoter. Full-length ATAF2 interacted with p*BAS1*-EE in a targeted Y1H assay (Fig. 1A). The CCA1 binding site (CBS; AAAAATCT or its complementary sequence) is similar to EE in sequence. Both EE and CBS are binding targets of the circadian clock protein CCA1 (Wang and Tobin, 1998; Michael and McClung, 2002; Harmer and Kay, 2005). As there are two CBSs in the *BAS1* promoter and one in the *SOB7* promoter (Pan et al., 2009), three CBS-containing promoter fragments (Table S1), p*BAS1*-CBS1 (−844 to −786), p*BAS1*-CBS2 (−1832 to −1768) and p*SOB7*-CBS (−1623 to −1524), were used as baits in targeted Y1H assays to test the hypothesis that ATAF2 binds the EE/CBS elements in the *BAS1* and *SOB7* promoters. CBS was the only predicted TF binding site in all three fragments when scanned with the Athena program. ATAF2 interacted with both p*BAS1*-CBS1 (Fig. 1B) and p*SOB7*-CBS (Fig. 1C).

An electrophoresis mobility shift assay (EMSA) provided additional evidence that ATAF2 interacts with a CBS-containing DNA fragment (Fig. 1D). ATAF2 bound with biotin-labeled p*BAS1*-CBS1, suggesting the formation of an ATAF2–p*BAS1*-CBS1 complex. With increasing concentrations of the unlabeled probes, the specific binding signal of p*BAS1*-CBS1 with ATAF2 was gradually abolished (Fig. 1D), which further suggests the physical interaction between ATAF2 and p*BAS1*-CBS1.

To further test whether the interaction between ATAF2 and the *BAS1*/*SOB7* promoters is mediated by the EE/CBS elements, site-directed mutagenesis was performed for both p*BAS1*-EE (the EE element was mutated from AAAATATCT to AACATATCT, named p*BAS1*-EEm) and p*SOB7*-CBS (the CBS element was mutated from AGATTTTT to AGATTCTT, named p*SOB7*-CBSm). Neither p*BAS1*-EEm (Fig. 1E) nor p*SOB7*-CBSm (Fig. 1F) was able to interact with ATAF2 in targeted Y1H assays, which indicates that the EE/CBS elements are responsible for the binding of ATAF2.

Additionally, neither ATAF2 nor ATAF2t protein showed interaction with p*BAS1*-CBS2 in the targeted Y1H assay (Fig. S1), which indicates that the existence of EE/CBS sequence alone is insufficient to mediate interaction with ATAF2.

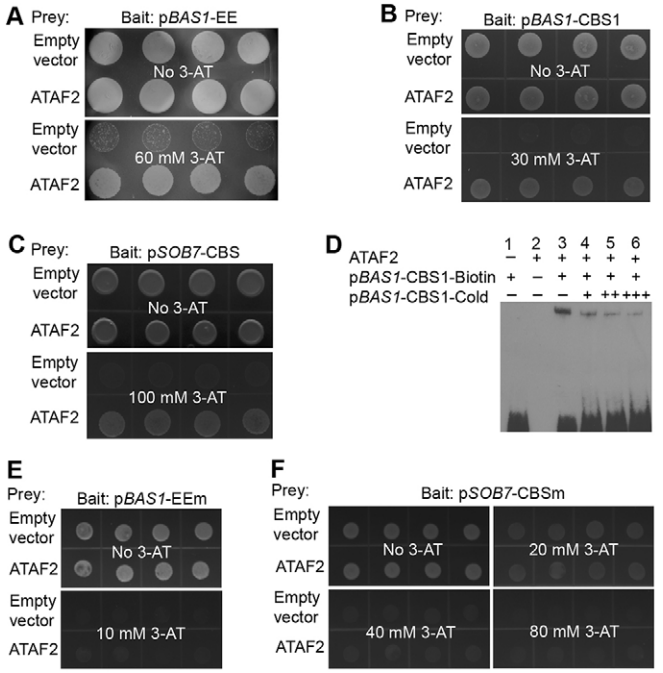

Fig. 1. ATAF2 binds to the promoters of *BAS1* and *SOB7*. (A-C) ATAF2 interacted with p*BAS1*-EE (A), p*BAS1*-CBS1 (B) and p*SOB7*-CBS (C) in a targeted Y1H assay. (D) ATAF2 bound to biotin-labeled p*BAS1*-CBS1 in an EMSA. (E) ATAF2 did not interact with p*BAS1*-EEm, in which the EE element has been mutated. (F) ATAF2 did not interact with p*SOB7*-CBSm, in which the CBS element has been mutated. For each tested Y1H interaction, yeast with the indicated bait sequence integrated in the genome was transformed with the indicated prey plasmids and plated on selection medium supplemented with 3-AT of the indicated concentrations. Four independent clones are shown for each sample. For EMSA, 20 fmol p*BAS1*-CBS1-biotin probe was used in the reaction (lanes 1, 3-6). With increasing concentrations of cold unlabeled p*BAS1*-CBS1 probe (4, 10 and 50 pmol in lanes 4, 5 and 6, respectively), the binding of ATAF2 protein to biotin-labeled p*BAS1*-CBS1 was gradually abolished.

ATAF2 suppresses the expression of *BAS1* and *SOB7*

ATAF2 can either activate (Wang et al., 2009; Huh et al., 2012) or suppress (Delessert et al., 2005) the expression of downstream target genes. To test the effects of ATAF2 on *BAS1* and *SOB7* expression, the transcript accumulation of *BAS1* and *SOB7* in *ATAF2* gain- and loss-of-function seedlings was examined by qRT-PCR (unless otherwise stated, 4-day-old seedlings grown at 25°C were used for all total RNA extraction and hypocotyl measurement experiments). *BAS1* transcript accumulation was significantly decreased in *ATAF2* overexpression (*ATAF2ox*) lines and increased in *ataf2* null mutants (*ataf2-1*, *ataf2-2*) in both darkness (Fig. 2A) and 80 µmol m^{-2} s^{-1} continuous white light (Fig. 2B). A similar relationship was observed in the case of *SOB7* transcript accumulation, except that *SOB7* expression in *ATAF2ox* seedlings was not significantly reduced in white light (Fig. 2C,D).

The effects of ATAF2 on the expression of BR biosynthesis genes were also tested. Unlike the BR-inactivation genes *BAS1* and *SOB7*, two key BR biosynthesis genes, *DWF4* (Choe et al., 1998) and *CPD* (Szekeres et al., 1996), did not show any dramatic changes of expression in the gain- or loss-of-function *ATAF2* mutants (Fig. S2A-D), which indicates that ATAF2 does not affect BR biosynthesis directly under the conditions tested. In darkness, the slight changes in *DWF4* and *CPD* transcript accumulation in loss- and gain-of-function *ATAF2* mutants (Fig. S2A,C) might be caused by transcriptional feedback regulation due to altered BR levels (Tanaka et al., 2005).

ATAF2 restricts the tissue-specific expression of BAS1 and SOB7 *in planta*

GUS analysis of ATAF2-GUS fusion transgenic *Arabidopsis* plants revealed that ATAF2 is expressed at varying levels in all plant tissues (Delessert et al., 2005). Similarly, GUS analysis showed that BAS1 and SOB7 have distinct, as well as overlapping, expression patterns and that these are limited to certain tissues, such as the shoot apex, root tip or root elongation zone (Sandhu et al., 2012). The

Development (2015) 142, 4129-4138 doi:10.1242/dev.124347

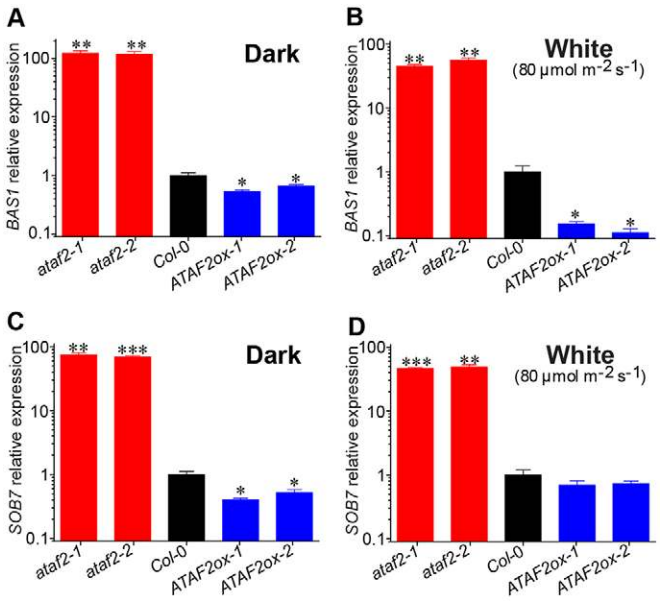

Fig. 2. ATAF2 suppresses the expression of *BAS1* and *SOB7*. *BAS1* accumulation was decreased in *ATAF2ox* seedlings and increased in *ataf2-1* and *ataf2-2* mutants under both dark (A) and 80 µmol m^{-2} s^{-1} white light (B) conditions, as was the case with *SOB7* accumulation in dark (C). In white light, only the *ataf2-1* and *ataf2-2* mutants showed significantly increased *SOB7* accumulation (D). Each qRT-PCR value is the mean of results from three biological replicates (n=3). Error bars denote the s.e.m. *P<0.05, **P<0.01, ***P<0.001 (unpaired one-tailed Student's t-test, versus control group of *Col*-0).

inconsistency of expression patterns between ATAF2 and BAS1/SOB7 proteins indicates that ATAF2 might function as an *in vivo* repressor to restrict the expression of BAS1 and SOB7 in specific tissues. To test this hypothesis, p*BAS1*:BAS1-GUS and p*SOB7*:SOB7-GUS (genomic DNA translational fusions with 1.6 and 2.1 kb of their native promoters, respectively) transgenes were expressed in the *ataf2-2* background. The *BAS1* promoter used includes the ATAF2 interaction-positive p*BAS1*-EE and p*BAS1*-CBS1 fragments, but not the ATAF2 interaction-negative p*BAS1*-CBS2 fragment. The *SOB7* promoter used includes the ATAF2 interaction-positive p*SOB7*-CBS element. Approximately 10% of the T1 primary transformants showed BR deficiency-associated dwarf (BR-dwarf) phenotypes for both transgenes (Fig. S3). Homozygous T3 plants were identified from the BR-dwarf single-locus T-DNA insertion lines for each transgene.

In order to compare the expression strength of exactly the same p*BAS1*:BAS1-GUS or p*SOB7*:SOB7-GUS genomic insertion sites in wild-type (*Col*-0) and *ataf2-2* backgrounds, these selected homozygous single-locus T-DNA insertion BR-dwarf lines were crossed with *Col*-0, and homozygous p*BAS1*:BAS1-GUS/*Col*-0, p*BAS1*:BAS1-GUS/*ataf2-2*, p*SOB7*:SOB7-GUS/*Col*-0 and p*SOB7*:SOB7-GUS/*ataf2-2* lines were identified from the segregating F2 populations. Whereas many p*BAS1*:BAS1-GUS/*ataf2-2* and p*SOB7*:SOB7-GUS/*ataf2-2* plants retained the BR-dwarf phenotype, no BR-dwarfs were identified in their p*BAS1*:BAS1-GUS/*Col*-0 and p*SOB7*:SOB7-GUS/*Col*-0 siblings (Fig. 3A,B). In addition, GUS analysis demonstrated that the disruption of *ATAF2* allowed the expansion of BAS1 and SOB7 expression to almost all plant tissues (Fig. 3C,D). In conclusion, the disruption of *ATAF2* dramatically increased the expression of BAS1 and SOB7 proteins, demonstrating its role as a negative regulator of these BR-inactivating enzymes.

ATAF2 loss- and gain-of-function seedlings have opposite BR-response phenotypes

The expression levels of *BAS1* and *SOB7* influence seedling growth in response to exogenous BRs (Neff et al., 1999; Turk et al., 2003, 2005; Thornton et al., 2010). As a transcriptional repressor of *BAS1* and *SOB7*, the expression level of *ATAF2* is also likely to influence seedling growth in response to exogenous BRs. To test this hypothesis, *Col*-0, the *ataf2* null and the *ATAF2ox* mutants were grown on media with gradient concentrations of BL (0, 10, 100 and 1000 nM) in darkness or 80 µmol m^{-2} s^{-1} white light. At all three BL concentrations, *Col*-0 hypocotyl growth was inhibited in darkness and enhanced in white light, which is consistent with the findings of Turk et al. (2003). When compared with *Col*-0, the *ataf2* null mutants were less responsive to all exogenous BL treatments, with longer hypocotyls in the dark and shorter hypocotyls in the light. By contrast, the *ATAF2ox* mutants generally displayed the opposite response of shorter hypocotyls in the dark and longer hypocotyls in the light (Fig. 4A-D), the only exception being that, in white light, *ATAF2ox* mutants only showed a significant hypocotyl growth phenotype with 100 nM BL treatment. These results indicate that 100 nM BL might be an ideal dose for the identification of hypocotyl elongation phenotypes for both dark and white light conditions.

Alteration of endogenous BR levels may also cause hypocotyl growth phenotypes in *ATAF2* mutants. When grown in the dark, *ataf2-1* and *ATAF2ox* seedlings showed opposite hypocotyl growth phenotypes in response to treatments with the BR biosynthesis inhibitor BRZ (Fig. 4E,F). In all three BRZ treatment conditions (20, 100 and 500 nM), BRZ slightly promoted hypocotyl growth of *Col*-0 and the *ATAF2ox* mutants, but inhibited that of *ataf2* null mutants. Upon BRZ treatment, *ataf2* null mutants always had a shorter hypocotyl than that of *Col*-0, whereas *ATAF2ox* mutants were always taller than *Col*-0. BRZ treatment assays further demonstrated that the hypocotyl growth phenotypes of *ATAF2* mutants are due to the changes in BR levels.

BRZ has been reported to inhibit the hypocotyl growth of dark-grown seedlings at lower temperatures (Asami et al., 2000; Nagata et al., 2000). Thus, the BRZ treatment assays were also conducted on dark-grown seedlings at 20°C (Fig. 4G). At this temperature, BRZ inhibited the hypocotyl growth of all three genotypes. *ATAF2ox* mutants were always less responsive to BRZ treatments than *Col*-0, whereas *ataf2* null mutants exhibited the opposite phenotype. When grown at 20°C, *ATAF2ox* mutants were shorter than both *Col*-0 and *ataf2* null mutants in the absence of BRZ.

Because ATAF2 has been reported to regulate the expression of the auxin biosynthesis gene *NIT2* (Huh et al., 2012), the involvement of auxin in ATAF2-mediated seedling phenotypes was tested, along with that of BRs. In contrast to the distinct hypocotyl growth phenotypes in *ATAF2* mutants caused by BL and BRZ, treatment with either auxin indole-3-acetic acid (IAA) or the auxin transport inhibitor naphthylphthalamic acid (NPA) (Ruegger et al., 1997) did not significantly affect the hypocotyl growth phenotypes of *ATAF2* loss- and gain-of-function seedlings in darkness (Fig. S4A,B). These results suggest that BRs are more important than auxins in ATAF2-mediated hypocotyl growth.

ATAF2 modulates root growth by regulating BR catabolism

In addition to hypocotyl elongation, root growth is another important parameter for measuring seedling development. Thus, the effects of ATAF2 on seedling primary and lateral root growth were examined by BRZ and NPA treatment. With no BRZ applied, *Col*-0, *ataf2* null and *ATAF2ox* mutants showed similar primary root

Development (2015) 142, 4129-4138 doi:10.1242/dev.124347

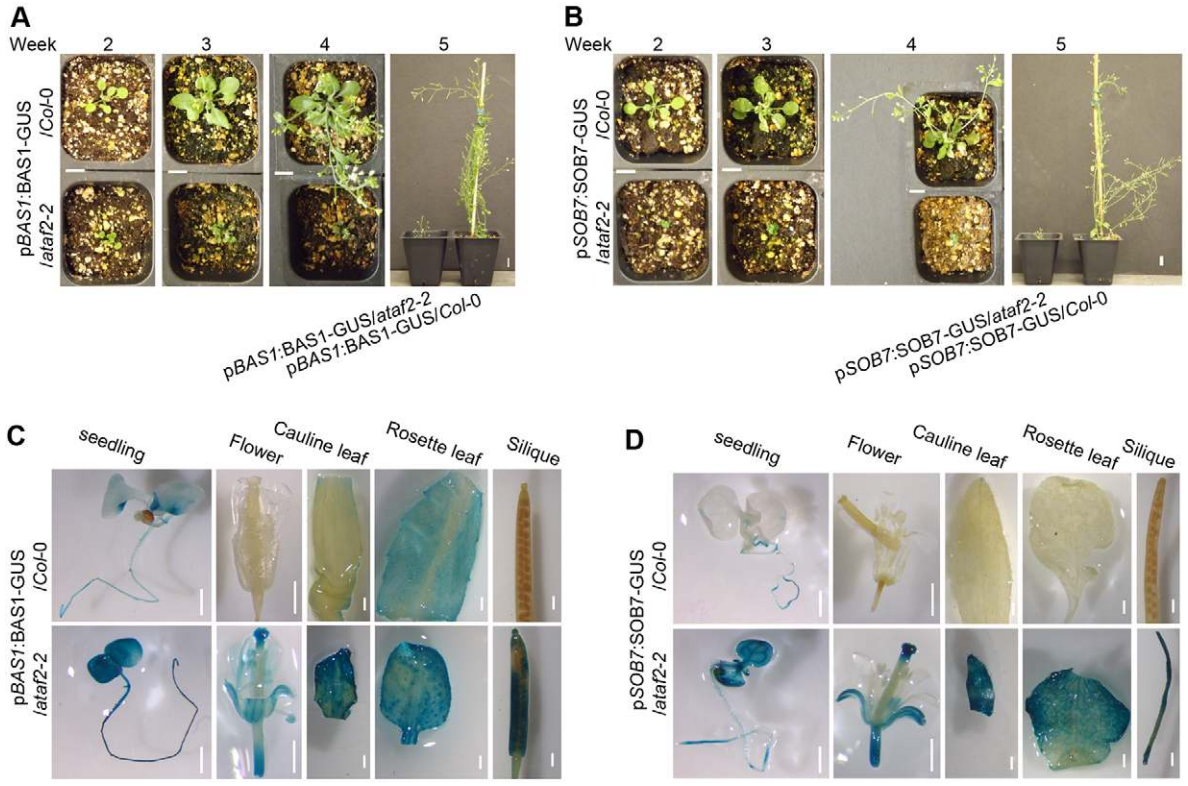

Fig. 3. ATAF2 restricts the tissue-specific expression of BAS1 and SOB7 *in planta*. Ectopic expression of p*BAS1*:BAS1-GUS and p*SOB7*:SOB7-GUS causes BR deficiency-associated dwarfism in *ataf2-2*. Single-locus T-DNA insertion p*BAS1*:BAS1-GUS/*ataf2-2* and p*SOB7*:SOB7-GUS/*ataf2-2* lines were crossed with *Col*-0. Homozygous lines were selected from the two F2 segregation populations for morphology comparison. (A) The p*BAS1*:BAS1-GUS/*ataf2-2* line was dwarf, whereas its p*BAS1*:BAS1-GUS/*Col*-0 sibling was relatively normal. (B) The p*SOB7*:SOB7-GUS/*ataf2-2* line was dwarf, whereas its p*SOB7*:SOB7-GUS/*Col*-0 sibling was relatively normal. (C,D) GUS analysis demonstrates that ATAF2 restricts the tissue-specific expression of BAS1 and SOB7 *in planta*. Scale bars: 1 cm in A,B; 1 mm in C,D.

growth (Fig. 5A). Compared with the wild type and *ATAF2ox* mutant, *ataf2-1* was more sensitive to exogenous BRZ treatments with respect to the elongation of the primary root (Fig. 5A). By contrast, *ataf2-1*, *Col*-0 and *ATAF2ox* seedlings showed similar primary root growth in response to exogenous NPA treatments (Fig. S5A), indicating that BRs are more important than auxins in ATAF2-mediated primary root growth regulation.

Even in the absence of BRZ, *ATAF2* loss- and gain-of-function seedlings showed opposite lateral root growth phenotypes (Fig. 5B). *ataf2-1* had more lateral root growth than *Col*-0, whereas overexpression of ATAF2 inhibited lateral root growth (Fig. 5B). Exogenous BRZ treatments significantly attenuated the lateral root growth phenotype of *ataf2-1*, but not that of *ATAF2ox* (Fig. 5B). With BRZ concentrations greater than 100 nM, the lateral root growth phenotype of *ataf2-1* was similar to that of the wild type. An NPA treatment assay was carried out in the presence of 100 nM BRZ to investigate whether disruption of auxin transport would cause a difference in lateral root growth between *Col*-0 and *ATAF2* mutants. The results showed that the lateral root growth phenotypes of *ataf2-1* and *ATAF2ox* under 100 nM BRZ were not significantly affected, compared with *Col*-0, by additional NPA treatments (Fig. S5B).

ATAF2 modulates hypocotyl growth in a fluence rate-dependent manner

In a fluence rate response assay (Fig. 6A,B), the hypocotyl growth of *ATAF2* loss- and gain-of-function and *Col*-0 seedlings showed no significant difference both in darkness and under high fluence rates of white light (80 and 100 µmol m^{-2} s^{-1}), which was consistent with observations above (Fig. 4A-D). However, *ATAF2* gain- and loss-of-function mutants displayed opposite hypocotyl length phenotypes in subsaturating fluence rates of white light (10, 20 and 40 µmol m^{-2} s^{-1}). Fluence rate response analysis demonstrated that ATAF2 stimulates hypocotyl growth in a light intensity-dependent manner (Fig. 6A,B). ATAF2 acts as a suppressor of seedling photomorphogenesis under subsaturating white light conditions.

The short-hypocotyl phenotype of *ataf2-1* under low fluence rate (10 µmol m^{-2} s^{-1}) white light was retained in monochromatic red (Fig. 6C), far-red (Fig. 6D) or blue (Fig. 6E) light. In order to investigate the contributions of photoreceptors to ATAF2-mediated photomorphogenesis, *ataf2-1* was crossed with null mutants of *PHYB*, *PHYA* and *CRY1* to create corresponding double mutants. Under the same fluence rate of monochromatic light (10 µmol m^{-2} s^{-1}), the short-hypocotyl phenotype of *ataf2-1* was retained but attenuated (Table S2) when knocking out *PHYB* (Fig. 6F), *PHYA* (Fig. 6G) or *CRY1* (Fig. 6H). These results indicate that ATAF2-mediated photomorphogenesis is regulated by multiple photoreceptors. Among the three photoreceptors examined, PHYA played the most significant role in regulating ATAF2-mediated seedling photomorphogenesis (Fig. 6D,G, Table S2).

In addition to far-red light, PHYA is known to respond to light in a wide range of wavelengths, including red (Tepperman et al., 2006; Franklin et al., 2007), blue and UV-A (Chun et al., 2001). Removal of PHYA was able to abolish the short-hypocotyl phenotype of *ataf2-1* under 10 µmol m^{-2} s^{-1} red (Fig. 6I) or blue (Fig. 6J) light.

Development (2015) 142, 4129-4138 doi:10.1242/dev.124347

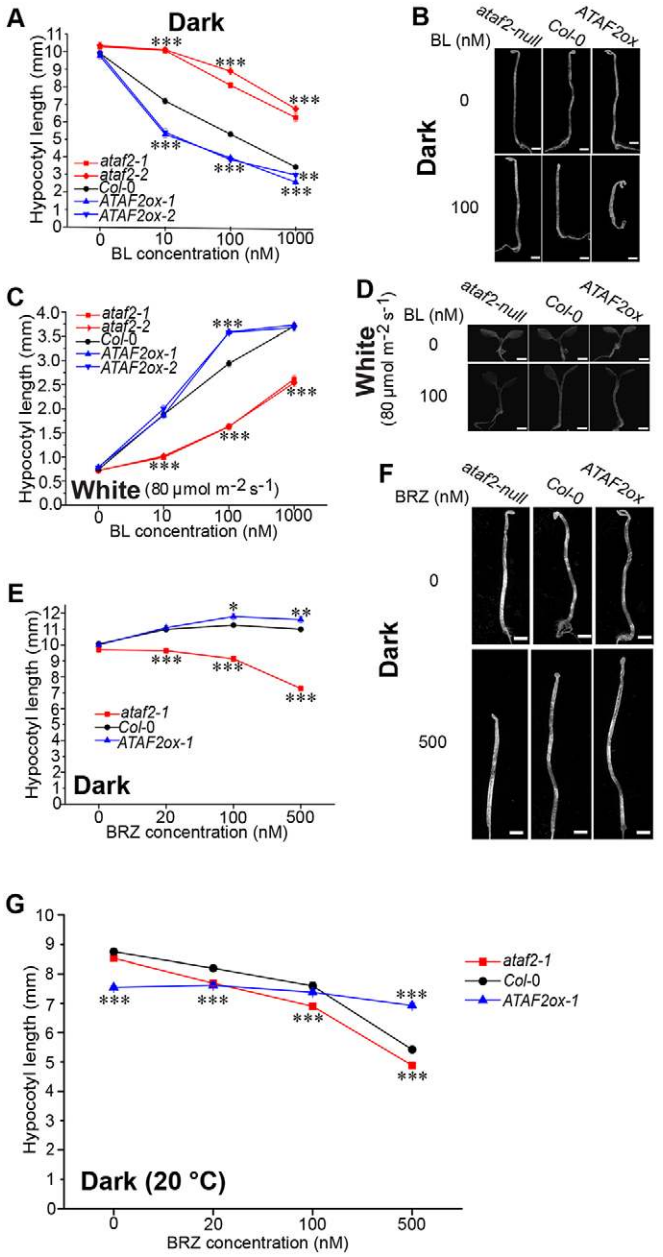

Fig. 4. *ATAF2* loss- and gain-of-function seedlings have opposite BR-response phenotypes. (A,B) In darkness, *ATAF2* loss- and gain-of-function seedlings exhibited BL-insensitivity and BL-oversensitivity phenotypes, respectively, under all three BL treatment conditions. (C,D) In white light, *ataf2-1* and *ataf2-2* seedlings had BL-insensitivity phenotypes under all three BL treatment conditions. *ATAF2ox* seedlings displayed significant BL-oversensitivity phenotypes only under treatment with 100 nM BL. (E-G) *ataf2-1* and *ATAF2ox* seedlings showed opposite hypocotyl growth phenotypes in response to BRZ treatments. Four-day-old seedlings were used for all the assays. The seedlings were grown at 25°C (A-F) or 20°C (G). (A,C,E,G) Each sample value represents the average of measurements from 30 seedlings (n=30). Error bars denote the s.e.m. *P<0.05, **P<0.01, ***P<0.001 (unpaired two-tailed Student's t-test, versus control group of *Col*-0); when a single significance level label is used for several similar genotypes, it means that all these samples have an identical significance level. Scale bars: 1 mm.

These results indicate that the regulatory function of PHYA in ATAF2-mediated photomorphogenesis operates in light conditions of various wavelengths.

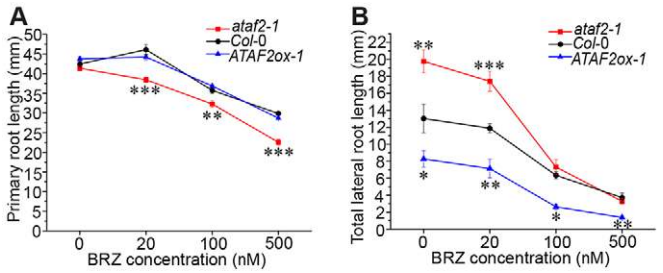

Fig. 5. *ATAF2* modulates root growth by regulating BR catabolism. (A) *ataf2-1* showed reduced primary root growth in response to exogenous BRZ treatments. (B) *ATAF2* loss- and gain-of-function seedlings showed opposite lateral root growth phenotypes. Exogenous BRZ treatments attenuated the lateral root growth phenotype of *ataf2-1*. Each sample value represents the average of measurements from ten 7-day-old seedlings (n=10). Error bars denote the s.e.m. *P<0.05, **P<0.01, ***P<0.001 (unpaired two-tailed Student's t-test, versus control group of *Col*-0).

ATAF2 is transcriptionally suppressed by both BRs and light

Since ATAF2-regulated hypocotyl growth was shown to involve both BRs and light, the effects of these pathways on *ATAF2* transcript accumulation were analyzed by qRT-PCR. Exogenous BL suppressed *ATAF2* transcript accumulation in *Col*-0 seedlings grown in both darkness and continuous white light (Fig. 7A,B). In *Col*-0 seedlings, *ATAF2* transcript accumulation was also suppressed by continuous white light in a fluence rate-dependent manner (Fig. 7C), with high fluence rates being more effective in suppressing *ATAF2* transcript accumulation. Additionally, a 1-h white light treatment for dark-grown seedlings was sufficient to significantly reduce *ATAF2* transcript accumulation (Fig. 7D). These results revealed that *ATAF2* is transcriptionally regulated by both BR and light signals. The white light-induced suppression of *ATAF2* accumulation was retained in the same fluence rate (10 µmol m^{-2} s^{-1}) of monochromatic red, far-red or blue light (Fig. 7E), which is consistent with ATAF2-mediated photomorphogenesis being regulated by multiple photoreceptors and with the major regulator, PHYA, functioning in a wide range of wavelengths.

The removal of PHYA did not affect *ATAF2* transcript accumulation in dark-grown seedlings (Fig. 7F). The light-induced suppression of *ATAF2* accumulation was attenuated by the removal of PHYA in 10 µmol m^{-2} s^{-1} white, red, far-red or blue light (Fig. 7G). This is also consistent with our observation that ATAF2-mediated photomorphogenesis is regulated by multiple photoreceptors, with PHYA playing a major role in light conditions of various wavelengths (Fig. 6A-J).

ATAF2 integrates BR catabolism and seedling photomorphogenesis

To test whether the ATAF2-mediated photomorphogenic phenotype is caused by changes in endogenous BR levels, *Col*-0 and *ATAF2* loss- and gain-of-function seedlings grown under low fluence rate (10 µmol m^{-2} s^{-1}) white light were treated with increasing concentrations (0, 20, 100 and 500 nM) of BRZ. Exogenous BRZ treatments attenuated the hypocotyl growth phenotypes of *ATAF2* loss- and gain-of-function seedlings (Fig. 8A,B). The addition of 500 nM BRZ was sufficient to eliminate the hypocotyl length differences of all three genotypes (Fig. 8A,B). By contrast, NPA treatments did not affect the hypocotyl growth phenotypes of *ATAF2* loss- and gain-of-function seedlings under identical light conditions (Fig. S6). BRZ and NPA response assays demonstrated that BRs play a more important role than auxins in ATAF2-mediated seedling photomorphogenesis.

Development (2015) 142, 4129-4138 doi:10.1242/dev.124347

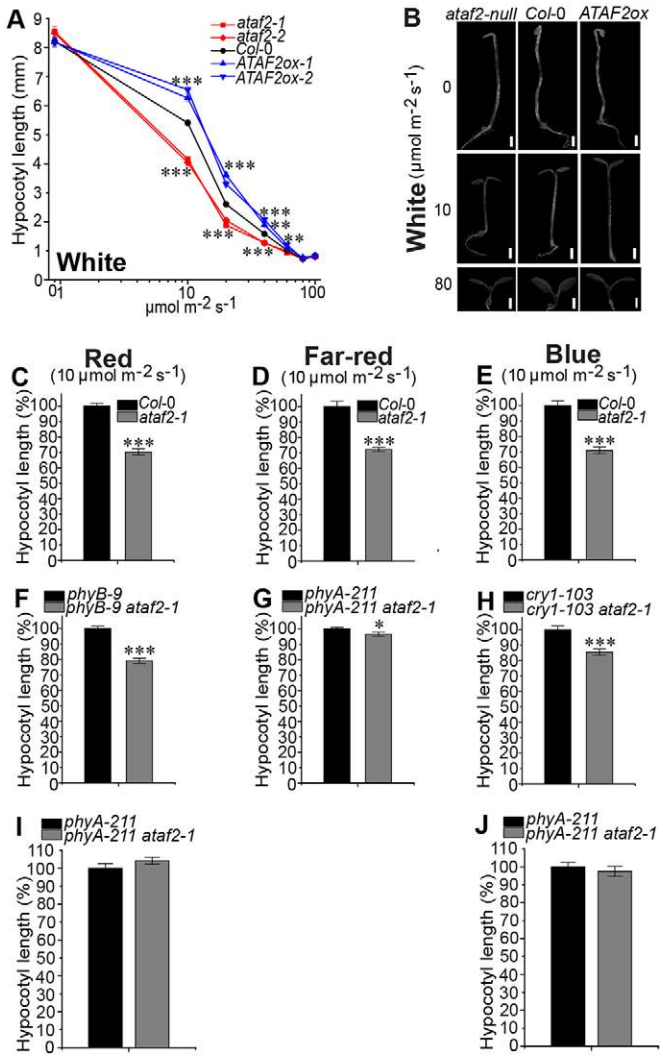

Fig. 6. *ATAF2* modulates hypocotyl growth in a fluence rate-dependent manner. (A,B) Increasing white light fluence rates attenuated the hypocotyl growth phenotype in both *ATAF2* loss- and gain-of-function mutant seedlings. (C-H) ATAF2-mediated photomorphogenesis is regulated by multiple photoreceptors. The short-hypocotyl phenotype of *ataf2-1* under low fluence rate (10 μmol m^{-2} s^{-1}) white light was retained in monochromatic red (C), far-red (D) or blue (E) light. Under the same fluence rate of monochromatic light, the short-hypocotyl phenotype of *ataf2-1* was retained but attenuated (Table S2) by the removal of *PHYB* (F), *PHYA* (G) or *CRY1* (H), with the removal of *PHYA* being the most dramatic. Removal of PHYA also abolished the short-hypocotyl phenotype of *ataf2-1* under 10 μmol m^{-2} s^{-1} red (I) or blue (J) light. (C-J) All measurements were from 3-day-old seedlings grown at 25°C. (A,C-J) Each sample value represents the average of measurements from 30 seedlings (*n*=30). Error bars denote the s.e.m. **P*<0.05, ***P*<0.01, ****P*<0.001 [unpaired two-tailed Student's *t*-test, versus the control group of *Col*-0 (A,C-E), of *phyB-9* (F), of *cry1-103* (H), or of *phyA-211* (G,I,J)]. When a single significance level label is used for several similar genotypes it indicates that the significance level is identical for these samples. Scale bars: 1 mm.

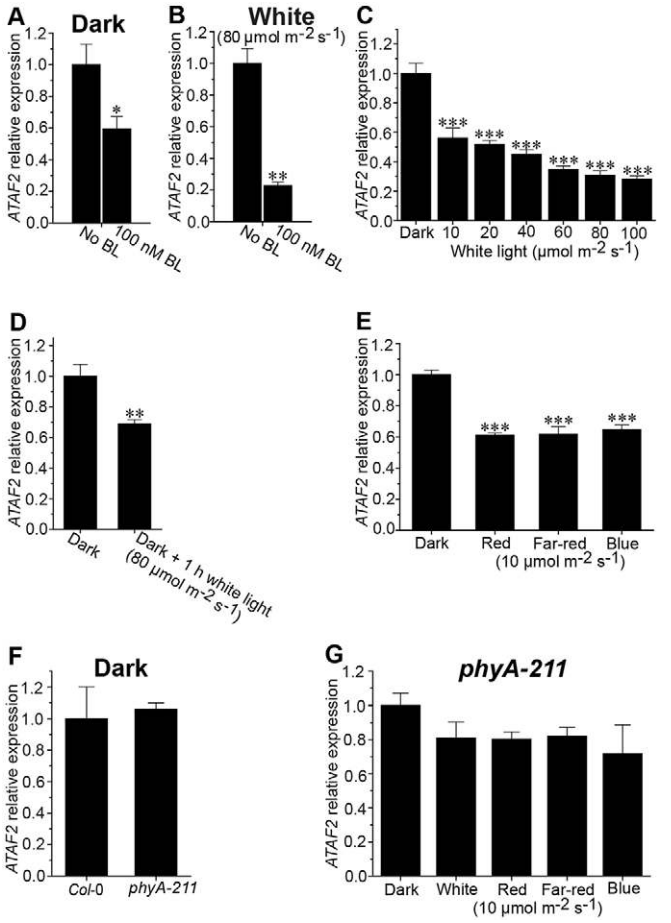

Fig. 7. *ATAF2* is transcriptionally suppressed by both BR and light signals. (A,B) In *Col*-0 seedlings, *ATAF2* accumulation was significantly suppressed by 100 nM BL treatment in both darkness (A) and white light (B). (C) *ATAF2* accumulation was suppressed by white light in a fluence rate-dependent manner. (D) *ATAF2* accumulation was significantly suppressed by 1-h treatment with white light. (E) The white light-induced suppression of *ATAF2* accumulation was retained in monochromatic red, far-red or blue light. (F) The removal of PHYA did not affect *ATAF2* transcript accumulation in dark-grown seedlings. (G) The light-induced suppression of *ATAF2* accumulation was attenuated by the removal of PHYA in 10 μmol m^{-2} s^{-1} white, red, far-red or blue light. Error bars denote the s.e.m. **P*<0.05, ***P*<0.01, ****P*<0.001 (unpaired one-tailed Student's *t*-test). (A,B) Each qRT-PCR value is the mean of results from three biological replicates (*n*=3), and *t*-tests were performed between the BL-treated sample group and the untreated control. (C-E) Each qRT-PCR value is the mean of results from six replicates (*n*=6; three biological replicates, each with two technical replicates), and *t*-tests were performed between the indicated sample group and the control group of *Col*-0 under dark conditions. (F) Each qRT-PCR value is the mean of results from three biological replicates (*n*=3), and *t*-tests were performed between the *phyA-211* group and the control group of *Col*-0 under dark conditions. (G) Each qRT-PCR value is the mean of results from three biological replicates (*n*=3), and *t*-tests were performed between the indicated sample group and the control group of *phyA-211* under dark conditions.

To test the function of *BAS1* and *SOB7* in the ATAF2-mediated photomorphogenic phenotype, a *bas1-2 sob7-1 ataf2-1* triple mutant was created and compared with the *bas1-2 sob7-1* double mutant for hypocotyl growth in response to different fluence rates (0, 10 and 80 μmol m^{-2} s^{-1}) of white light (Fig. 8C). Removal of *BAS1* and *SOB7* completely abolished the short-hypocotyl phenotype caused by disruption of *ATAF2* (Fig. 8C). This indicates that ATAF2 suppresses seedling photomorphogenesis by repressing expression of the BR-inactivation genes *BAS1* and *SOB7* (Fig. 8D).

DISCUSSION

ATAF2 binds A/T-rich *cis*-acting elements to regulate the activities of downstream genes

ATAF2 is an NAC family TF that is localized in the nucleus (Wang et al., 2009). NAC TFs have a highly conserved N-terminal NAC domain and diverse C-terminal domains. The NAC domain can bind both DNA and protein. The C-terminal domains are responsible for the activation or suppression of downstream target genes (Ernst et al., 2004). ATAF2 has been reported to bind a 25 bp A/T-rich

Development (2015) 142, 4129-4138 doi:10.1242/dev.124347

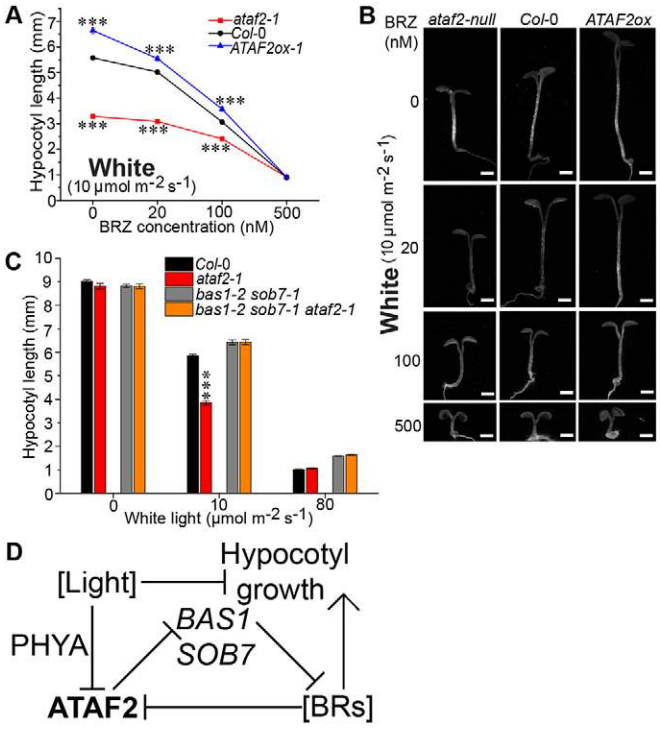

Fig. 8. ATAF2 integrates BR catabolism and seedling photomorphogenesis. (A,B) Exogenous BRZ treatments attenuated the hypocotyl growth phenotypes of *ATAF2* loss- and gain-of-function seedlings under low fluence rate (10 µmol m^{-2} s^{-1}) white light. (C) There were no significant differences in hypocotyl lengths between the *bas1-2 sob7-1* double mutant and the *bas1-2 sob7-1 ataf2-1* triple mutant in response to different fluence rates (0, 10 and 80 µmol m^{-2} s^{-1}) of white light. Four-day-old seedlings grown at 25°C were used for all the assays. (A,C) Each sample value represents the average of measurements from 30 seedlings (*n*=30). Error bars denote the s.e.m. ***P<0.001 (unpaired two-tailed Student's *t*-test). *t*-tests were performed (A) between the indicated sample group and the control group of *Col*-0 or (C) between either the *ataf2-1* group and the control group of *Col-0*, or the *bas1-2 sob7-1 ataf2-1* group and the control group of *bas1-2 sob7-1*. (D) Model of ATAF2 function in connecting hypocotyl growth to BR catabolism and light fluence rates. ATAF2 promotes hypocotyl growth by elevating the BR level in seedlings, which is accomplished by suppressing expression of the BR-inactivating genes *BAS1* and *SOB7*. BRs suppress *ATAF2* expression to form a feedback regulation loop. White light suppresses hypocotyl growth through multiple pathways. One of which is by suppressing *ATAF2* to modulate BR catabolism. Scale bars: 1 mm.

consensus sequence (Wang and Culver, 2012) and a 36 bp A/T-rich sequence (Huh et al., 2012). Here, we have shown that ATAF2 also binds the A/T-rich EE/CBS elements (Fig. 1A-F). Interestingly, ATAF2 interacts with two members of the AT-hook motif-containing nuclear-localized (AHL) protein family, which specifically bind A/T-rich DNA (Zhao et al., 2013). The similarity in binding targets between ATAF2 and AHLs might facilitate their interaction *in vivo*. AHLs are present in all plant species and are involved in a wide range of biological processes, including the regulation of *Arabidopsis* hypocotyl growth (Zhao et al., 2013, 2014). Together, these observations suggest that ATAF2 and certain AHL proteins might work as functional partners in this fundamental plant development process.

The observation that ATAF2 and CCA1 share common promoter binding sites indicates that they might interact *in vivo* to regulate downstream gene expression coordinately (binding together to function) or antagonistically (competing for the same binding site or restricting each other from binding targets by direct protein-protein interaction). There is also a putative CBS (−577 to −570) in the *ATAF2* promoter, which suggests that CCA1 might also regulate the expression of *ATAF2* by directly binding its promoter.

Recently, more than 1000 CCA1 binding regions were identified via the ChIP-seq approach (Nagel et al., 2015), although the *BAS1*, *SOB7* and *ATAF2* promoters were not identified as CCA1 targets. Nagel et al. (2015) used 10-day-old *Arabidopsis* plants, whereas we used 3- to 4-day-old seedlings. The age difference and/or growth conditions might explain the differences between the two studies. In addition, the ChIP-seq approach might not identify all CCA1 binding sites, especially those where binding is transient or weak.

ATAF2 is indispensable for the spatial regulation of BR homeostasis

ATAF2 acts as a repressor of *BAS1* and *SOB7* expression (Fig. 2A-D). *ATAF2* expression is suppressed by BRs (Fig. 7A,B). Therefore, ATAF2-BAS1/SOB7-BR-ATAF2 forms a feedback regulation loop. The BR biosynthesis genes *DWF4* and *CPD* are not involved in this ATAF2 regulatory loop in our growth conditions (Fig. S2A-D). This is consistent with the fact that no EE/CBS element is detected when a 2.5 kb region of the *DWF4* or *CPD* promoter is scanned with the Athena program. In addition to transcriptionally repressing *BAS1* and *SOB7*, the emergence of BR-deficient dwarf plants in p*BAS1*:BAS1-GUS/*ataf2-2* and p*SOB7*:SOB7-GUS/*ataf2-2* transgenic populations (Fig. 3A,B, Fig. S3) indicates that the disruption of *ATAF2* dramatically increases the expression of BAS1 and SOB7 proteins. In addition, comparison of identical p*BAS1*:BAS1-GUS and p*SOB7*:SOB7-GUS transgene insertions in *Col*-0 and *ataf2-2* backgrounds supports the hypothesis that ATAF2 modulates the expression patterns of BAS1 and SOB7, restricting their expression to certain tissues, and controlling their expression within certain levels (Fig. 3C,D).

Although some p*BAS1*:BAS1-GUS/*ataf2-2* and p*SOB7*:SOB7-GUS/*ataf2-2* transgenic plants have BR-dwarf phenotypes, the original *ataf2-2* mutant is not dwarf. There are at least four possible explanations for these observations. First, the transgenic plants harbor additional copies of *BAS1* or *SOB7*. Second, the genomic positions of the transgenes differ from those of endogenous *BAS1* or *SOB7*. Third, remote *cis*-regulatory elements might not be included in the promoter regions cloned in the constructs. Fourth, the fusion of ATAF2 to GUS protein might help to stabilize ATAF2. In *Arabidopsis*, there are examples in which GUS and GFP tags increase the stability of several SMALL AUXIN UP RNA (SAUR) proteins (Chae et al., 2012; Spartz et al., 2012). In this case, BAS1-GUS or SOB7-GUS translational fusion proteins might have greater stability than native BAS1 or SOB7, and the increased accumulation of BAS1-GUS or SOB7-GUS might lead to the BR-deficient dwarf phenotypes in p*BAS1*:BAS1-GUS/*ataf2-2* or p*SOB7*:SOB7-GUS/*ataf2-2*, respectively. In conclusion, any of the possible reasons mentioned above could result in sufficient expression of BAS1 or SOB7 in transgenic *ataf2-2* to cause the dwarf phenotype due to increased BR inactivation.

The GUS expression patterns in p*BAS1*:BAS1-GUS/*Col*-0 and p*SOB7*:SOB7-GUS/*Col*-0 are similar, but not exactly identical to, those reported previously (Sandhu et al., 2012), which might also be a consequence of differences in T-DNA insertion position among ectopic expression lines. Additionally, differences in the genetic background might affect the GUS expression pattern observed. Wild-type (*Col*-0) plants were used to generate GUS expression lines in this work, whereas Sandhu et al. (2012) adopted a *bas1-2 sob7-1* double-mutant background for p*BAS1*:BAS1-GUS and p*SOB7*:SOB7-GUS expression.

Development (2015) 142, 4129-4138 doi:10.1242/dev.124347

The hypocotyl growth phenotypes of *ATAF2* mutants can be triggered by either BR or light signals

The BL and BRZ response assay results (Fig. 4A-G) further support the hypothesis that ATAF2 acts as a repressor of BR catabolism. The reduced *ATAF2* expression in *ataf2* null mutants leads to higher transcript accumulation of *BAS1* and *SOB7*, which enhances the BR inactivation capacity in seedlings and confers more resistance to BL treatment. Conversely, higher expression of *ATAF2* in *ATAF2ox* mutants leads to lower levels of *BAS1* and *SOB7* transcript accumulation, which reduces the BR inactivation capacity in these seedlings, conferring more sensitivity to BL treatment. In darkness, *ATAF2ox* seedlings show a BL-oversensitivity phenotype under all three BL treatment conditions (Fig. 4A,B). In white light, a high concentration of exogenous BL (1 µM) masks the BL-oversensitivity phenotype of *ATAF2ox* seedlings. A low concentration of exogenous BL (10 nM) is not sufficient to induce the phenotype (Fig. 4C,D). However, the hypocotyl phenotype was evident upon treatment with 100 nM BL (Fig. 4C,D). Both *ataf2* null mutants had BL-insensitivity phenotypes under all six light- and dark-grown BL treatment conditions (Fig. 4A-D).

The relationship between BRs and the hypocotyl growth phenotypes of *ATAF2* mutants was further demonstrated by BRZ response analysis (Fig. 4E-G). In our assays, BRZ promotes the hypocotyl elongation of dark-grown seedlings (except *ATAF2* loss-of-function mutants) at 25°C (Fig. 4E,F) but inhibits the elongation at 20°C (Fig. 4G). This observation suggests that the sensitivity of dark-grown hypocotyls to endogenous BR levels is temperature dependent. Gray et al. (1998) reported that high temperature promotes hypocotyl elongation that is mainly mediated by auxin, with a lesser involvement of BRs.

In all the BR, BRZ and NPA treatment assays conducted, only two distinct light conditions (darkness and 80 µmol m^{-2} s^{-1} white light) were used. These two conditions were selected because all hypocotyl lengths were similar for the non-treatment controls, which facilitated the evaluation of BR treatment effects. Since it is well known that seedling photomorphogenesis is modulated by the coordination of light and hormonal signals, the involvement of light intensity and quality in ATAF2-regulated seedling growth was investigated. The fluence rate response assay demonstrates that ATAF2 stimulates hypocotyl growth in a light intensity-dependent manner (Fig. 6A,B). In darkness, the hypocotyl growth regulatory activity of ATAF2 was not significantly apparent. Under high fluence rates of white light, the light intensities were strong enough to suppress the photomorphogenic activities of ATAF2.

ATAF2 transcript accumulation is suppressed by light in a fluence rate-dependent manner (Fig. 7C,D), which at least partially explains why *ATAF2* loss- and gain-of-function and *Col*-0 seedlings have no significant difference in hypocotyl length under high fluence rates of light. ATAF2 has been reported to activate the expression of the auxin biosynthesis gene *NIT2* (Huh et al., 2012). Thus, both BRs and auxins could be involved in the photomorphogenic phenotypes of *ATAF2* mutants. BRZ (Fig. 8A,B) and NPA (Fig. S6) response assays demonstrate that BRs have a more important role in this response than auxins. The short-hypocotyl phenotype of *ATAF2* loss-of-function mutants relies on the expression of *BAS1* and *SOB7* (Fig. 8C), which further demonstrates that ATAF2-mediated photomorphogenic phenotypes depend on BR inactivation catalyzed by BAS1 and SOB7. Together, these results demonstrate the presence of a light-ATAF2-BAS1/SOB7-BR-photomorphogenesis signaling network. The BL-response phenotypes of *ATAF2ox* seedlings were more dramatic in darkness than in white light (Fig. 4A-D). These results provide indirect evidence that light-mediated reduction of *ATAF2* expression may attenuate ATAF2-mediated BR-response phenotypes.

Multiple photoreceptors regulate ATAF2-mediated photomorphogenesis, with PHYA playing a major role

ATAF2 loss- and gain-of-function seedlings retain their hypocotyl length phenotypes in monochromatic red, far-red and blue light (Fig. 6C-E). The phenotypes are attenuated (Fig. 6F-H, Table S2) by the removal of *PHYB*, *PHYA* or *CRY1*, with disruption of *PHYA* being the most dramatic (Fig. 6D,G, Table S2). These results suggest that multiple photoreceptors are involved in ATAF2-mediated seedling photomorphogenesis, with PHYA playing an important role. Turk et al. (2003) reported that the interaction between light and the BAS1-mediated BR-inactivation pathway is mainly dependent on far-red light. The regulation of ATAF2-mediated photomorphogenesis is consistent with this previous observation and might constitute part of the light-BR intersection. The observation that the ATAF2-mediated photomorphogenic phenotype under monochromatic red or blue light also requires PHYA (Fig. 6I,J) further demonstrates the close relationship between PHYA and ATAF2 function.

ATAF2 regulates root growth in part via BR catabolism

BRZ treatments reduce both primary and lateral root growth (Fig. 5A,B), which is consistent with previous observations that BRs can promote the growth of both tissues (Müssig et al., 2003; Bao et al., 2004). There have been numerous reports revealing the complexity of BR activity in controlling root growth and development (Hacham et al., 2011; Fridman et al., 2014; Vragović et al., 2015). BRZ (Fig. 5A,B) and NPA (Fig. S5A,B) response assays demonstrate that BRs are responsible for the primary and lateral root growth phenotypes modulated by ATAF2. The root phenotypes of *ATAF2* loss-of-function mutants indicate that this TF acts as a repressor of lateral root growth while acting as an activator of primary root growth in the presence of BRZ. Thus, it is possible that ATAF2 has a role in determining resource allocation and differential growth between the primary and lateral roots.

ATAF2 integrates *Arabidopsis* BR inactivation and seedling photomorphogenesis

Overall, we propose that ATAF2 acts as an integrator of BR catabolism and seedling photomorphogenesis (Fig. 8D). ATAF2 suppresses expression of the BR-inactivating genes *BAS1* and *SOB7*. As a result, ATAF2 promotes the elevation of BR levels. In turn, BRs suppress *ATAF2* expression to form an ATAF2-BAS1/SOB7-BR-ATAF2 feedback regulation loop. On the other hand, ATAF2 promotes hypocotyl growth at least partially via the pathway of BAS1/SOB7-mediated BR degradation. Light suppresses hypocotyl growth through multiple pathways, one of which is by suppressing *ATAF2* in a fluence rate-dependent manner. PHYA plays a major role in the ATAF2-mediated seedling photomorphogenic pathway. In this model, ATAF2 plays a key role in connecting seedling development with BR homeostasis and photomorphogenesis. Given that ATAF2 was previously reported to regulate plant defense (Delessert et al., 2005; Wang et al., 2009) and auxin biosynthesis (Huh et al., 2012), ATAF2 acts as a central regulator of plant defense, hormone metabolism and light-mediated seedling development.

MATERIALS AND METHODS

Plant materials

Arabidopsis plants used in this study are in the Columbia (*Col*-0) background. T-DNA insertion mutants were obtained from the

Development (2015) 142, 4129-4138 doi:10.1242/dev.124347

Arabidopsis Biological Resource Center (ABRC). For *ataf2-1* (SALK_136355), the T-DNA insertion site is in the second exon; for *ataf2-2* (SALK_015750), the T-DNA is located in the second intron. Quantitative RT-PCR (qRT-PCR) analysis (see below) demonstrated that both *ataf2-1* and *ataf2-2* are null alleles. For the generation of *ATAF2ox* lines, the *ATAF2* coding sequence was overexpressed in *Col*-0 under the control of the CaMV *35S* promoter. The p*BAS1*:BAS1-GUS and p*SOB7*:SOB7-GUS constructs were described previously (Turk et al., 2003; Sandhu et al., 2012). Homozygous single-locus T-DNA insertion lines were selected for all three transgenic events. The histochemical GUS analysis was described previously (Sandhu et al., 2012). Photoreceptor mutants (all in the *Col*-0 background) *phyB-9* (Reed et al., 1993), *phyA-211* (Reed et al., 1994) and *cry1-103* (Liscum and Hangarter, 1991) were crossed with *ataf2-1* to isolate double mutants with *ataf2-1* from F2 populations. The *bas1-2 sob7-1* double mutant (Turk et al., 2005) was crossed with *ataf2-1* to isolate the *bas1-2 sob7-1 ataf2-1* triple mutant. Identification by PCR of *bas1-2*, *sob7-1*, *phyB-9*, *phyA-211* and *cry1-103* mutations was described previously (Turk et al., 2005; Ward et al., 2005; Sandhu et al., 2012). Unless otherwise stated, 4-day-old seedlings were used for total RNA extraction and hypocotyl measurements, and 7-day-old seedlings were used for root growth measurements. Unless otherwise stated, seedlings were grown in growth chambers at 25°C for all physiological and molecular assays.

DNA-protein interaction assays

The Y1H assays were carried out using the Gateway-compatible system (Deplancke et al., 2006). Briefly, the promoter DNA fragments (baits) were amplified and fused to the reporter gene *HIS3*, and then integrated into the yeast genome. The yeast bait clones with the lowest self-activation levels were selected independently for each assay and used to either screen an *Arabidopsis* cDNA library for interacting protein prey or to test interactions with the targeted prey. The activation of *HIS3* was tested by yeast tolerance to 3-aminotriazole (3-AT, a competitive inhibitor of the His3p enzyme). Sequences of DNA fragments used for the Y1H screen and targeted Y1H are listed in Table S1. All constructs used in this research that were generated by PCR were sequence verified. Site-directed mutagenesis of baits was performed using the QuikChange Lightning Kit (Agilent Technologies). His-tagged ATAF2 protein was purified for EMSA by procedures described previously (Zhao et al., 2013).

Transcript analysis

Total RNA was extracted using the RNeasy Plant Kit (Qiagen). On-column DNase digestion was performed to eliminate genomic DNA contamination. Total cDNA was synthesized using the SuperScript III First-Strand Synthesis System (Invitrogen). qRT-PCR reactions were performed using SsoFast EvaGreen Supermix with the Low Rox Kit (Bio-Rad) and the 7500 Fast Real-Time PCR System (Applied Biosystems). Relative expression levels were determined by normalizing to the transcript levels of *UBQ10*. For each qRT-PCR assay, 4-day-old seedlings of three biological replicates were grown under the same treatment conditions at the same time. qRT-PCR primers are listed in Table S3.

Hypocotyl and root measurements

Seed sterilization, media composition, plating, growth conditions and hypocotyl measurement were as previously described (Sandhu et al., 2012; Zhao et al., 2013). For BL (Turk et al., 2003), BRZ (Asami et al., 2000), IAA (Collett et al., 2000) and NPA (Ruegger et al., 1997) treatment assays, seeds were put on the treatments from the beginning of the experiments. The 30 tallest seedlings from the group of three independent replicates were used for each sample in all hypocotyl measurements. For root growth measurement, seedlings were grown on vertical plates in white light. Ten seedlings with the longest primary or lateral root growth from the group of three independent replicates were used for each sample in all the root measurements. All seedlings were scanned/photographed and measured using NIH ImageJ (Schneider et al., 2012).

Acknowledgements

We thank Dr Hanjo Hellmann (Washington State University) for providing the *Arabidopsis* cDNA prey library.

Competing interests

The authors declare no competing or financial interests.

Author contributions

H.P., J.Z. and M.M.N. designed the experiments, analyzed the data and wrote the manuscript. J.Z. performed the EMSA. H.P. performed all the other experiments.

Funding

This research was supported by the United States National Science Foundation [project 1124749 to M.M.N.], and by the USDA National Institute of Food and Agriculture [HATCH project 1007178 to M.M.N.].

Supplementary information

Supplementary information available online at
http://dev.biologists.org/lookup/suppl/doi:10.1242/dev.124347/-/DC1

References

Asami, T., Min, Y. K., Nagata, N., Yamagishi, K., Takatsuto, S., Fujioka, S., Murofushi, N., Yamaguchi, I. and Yoshida, S. (2000). Characterization of brassinazole, a triazole-type brassinosteroid biosynthesis inhibitor. *Plant Physiol.* **123**, 93-100.

Bao, F., Shen, J., Brady, S. R., Muday, G. K., Asami, T. and Yang, Z. (2004). Brassinosteroids interact with auxin to promote lateral root development in Arabidopsis. *Plant Physiol.* **134**, 1624-1631.

Belkhadir, Y., Jaillais, Y., Epple, P., Balsemão-Pires, E., Dangl, J. L. and Chory, J. (2012). Brassinosteroids modulate the efficiency of plant immune responses to microbe-associated molecular patterns. *Proc. Natl. Acad. Sci. USA* **109**, 297-302.

Bell, E. M., Lin, W.-c., Husbands, A. Y., Yu, L., Jaganatha, V., Jablonska, B., Mangeon, A., Neff, M. M., Girke, T. and Springer, P. S. (2012). Arabidopsis lateral organ boundaries negatively regulates brassinosteroid accumulation to limit growth in organ boundaries. *Proc. Natl. Acad. Sci. USA* **109**, 21146-21151.

Chae, K., Isaacs, C. G., Reeves, P. H., Maloney, G. S., Muday, G. K., Nagpal, P. and Reed, J. W. (2012). Arabidopsis *SMALL AUXIN UP RNA63* promotes hypocotyl and stamen filament elongation. *Plant J.* **71**, 684-697.

Choe, S., Dilkes, B. P., Fujioka, S., Takatsuto, S., Sakurai, A. and Feldmann, K. A. (1998). The *DWF4* gene of Arabidopsis encodes a cytochrome P450 that mediates multiple 22 α-hydroxylation steps in brassinosteroid biosynthesis. *Plant Cell* **10**, 231-243.

Chory, J., Peto, C., Feinbaum, R., Pratt, L. and Ausubel, F. (1989). *Arabidopsis thaliana* mutant that develops as a light-grown plant in the absence of light. *Cell* **58**, 991-999.

Chory, J., Nagpal, P. and Peto, C. A. (1991). Phenotypic and genetic analysis of *det2*, a new mutant that affects light-regulated seedling development in Arabidopsis. *Plant Cell* **3**, 445-459.

Chun, L., Kawakami, A. and Christopher, D. A. (2001). Phytochrome A mediates blue light and UV-A-dependent chloroplast gene transcription in green leaves. *Plant Physiol.* **125**, 1957-1966.

Collett, C. E., Harberd, N. P. and Leyser, O. (2000). Hormonal interactions in the control of Arabidopsis hypocotyl elongation. *Plant Physiol.* **124**, 553-562.

Delessert, C., Kazan, K., Wilson, I. W., Van Der Straeten, D., Manners, J., Dennis, E. S. and Dolferus, R. (2005). The transcription factor ATAF2 represses the expression of pathogenesis-related genes in Arabidopsis. *Plant J.* **43**, 745-757.

Deplancke, B., Vermeirssen, V., Arda, H. E., Martinez, N. J. and Walhout, A. J. M. (2006). Gateway-compatible yeast one-hybrid screens. *Cold Spring Harb. Protoc.* **2006**, pdb.prot4590.

Ernst, H. A., Nina Olsen, A., Skriver, K., Larsen, S. and Lo Leggio, L. (2004). Structure of the conserved domain of ANAC, a member of the NAC family of transcription factors. *EMBO Rep.* **5**, 297-303.

Franklin, K. A., Allen, T. and Whitelam, G. C. (2007). Phytochrome A is an irradiance-dependent red light sensor. *Plant J.* **50**, 108-117.

Fridman, Y., Elkouby, L., Holland, N., Vragović, K., Elbaum, R. and Savaldi-Goldstein, S. (2014). Root growth is modulated by differential hormonal sensitivity in neighboring cells. *Genes Dev.* **28**, 912-920.

Gray, W. M. (2004). Hormonal regulation of plant growth and development. *PLoS Biol.* **2**, e311.

Gray, W. M., Ostin, A., Sandberg, G., Romano, C. P. and Estelle, M. (1998). High temperature promotes auxin-mediated hypocotyl elongation in Arabidopsis. *Proc. Natl. Acad. Sci. USA* **95**, 7197-7202.

Guo, Z., Fujioka, S., Blancaflor, E. B., Miao, S., Gou, X. and Li, J. (2010). TCP1 modulates brassinosteroid biosynthesis by regulating the expression of the key biosynthetic gene *DWARF4* in *Arabidopsis thaliana*. *Plant Cell* **22**, 1161-1173.

Hacham, Y., Holland, N., Butterfield, C., Ubeda-Tomas, S., Bennett, M. J., Chory, J. and Savaldi-Goldstein, S. (2011). Brassinosteroid perception in the epidermis controls root meristem size. *Development* **138**, 839-848.

Harmer, S. L. and Kay, S. A. (2005). Positive and negative factors confer phase-specific circadian regulation of transcription in Arabidopsis. *Plant Cell* **17**, 1926-1940.

Huh, S. U., Lee, S.-B., Kim, H. H. and Paek, K.-H. (2012). ATAF2, a NAC transcription factor, binds to the promoter and regulates *NIT2* gene expression involved in auxin biosynthesis. *Mol. Cells* **34**, 305-313.
Li, J., Nagpal, P., Vitart, V., McMorris, T. C. and Chory, J. (1996). A role for brassinosteroids in light-dependent development of Arabidopsis. *Science* **272**, 398-401.
Liscum, E. and Hangarter, R. P. (1991). Arabidopsis mutants lacking blue light-dependent inhibition of hypocotyl elongation. *Plant Cell* **3**, 685-694.
Michael, T. P. and McClung, C. R. (2002). Phase-specific circadian clock regulatory elements in Arabidopsis. *Plant Physiol.* **130**, 627-638.
Müssig, C., Shin, G.-H. and Altmann, T. (2003). Brassinosteroids promote root growth in Arabidopsis. *Plant Physiol.* **133**, 1261-1271.
Nagata, N., Min, Y. K., Nakano, T., Asami, T. and Yoshida, S. (2000). Treatment of dark-grown *Arabidopsis thaliana* with a brassinosteroid-biosynthesis inhibitor, brassinazole, induces some characteristics of light-grown plants. *Planta* **211**, 781-790.
Nagel, D. H., Doherty, C. J., Pruneda-Paz, J. L., Schmitz, R. J., Ecker, J. R. and Kay, S. A. (2015). Genome-wide identification of CCA1 targets uncovers an expanded clock network in Arabidopsis. *Proc. Natl. Acad. Sci. USA* **112**, E4802-E4810.
Neff, M. M. and Chory, J. (1998). Genetic interactions between phytochrome A, phytochrome B, and cryptochrome 1 during Arabidopsis development. *Plant Physiol.* **118**, 27-35.
Neff, M. M., Nguyen, S. M., Malancharuvil, E. J., Fujioka, S., Noguchi, T., Seto, H., Tsubuki, M., Honda, T., Takatsuto, S., Yoshida, S. et al. (1999). *BAS1*: a gene regulating brassinosteroid levels and light responsiveness in Arabidopsis. *Proc. Natl. Acad. Sci. USA* **96**, 15316-15323.
Neff, M. M., Fankhauser, C. and Chory, J. (2000). Light: an indicator of time and place. *Genes Dev.* **14**, 257-271.
O'Connor, T. R., Dyreson, C. and Wyrick, J. J. (2005). Athena: a resource for rapid visualization and systematic analysis of Arabidopsis promoter sequences. *Bioinformatics* **21**, 4411-4413.
Pan, Y., Michael, T. P., Hudson, M. E., Kay, S. A., Chory, J. and Schuler, M. A. (2009). Cytochrome P450 monooxygenases as reporters for circadian-regulated pathways. *Plant Physiol.* **150**, 858-878.
Reed, J. W., Nagpal, P., Poole, D. S., Furuya, M. and Chory, J. (1993). Mutations in the gene for the red/far-red light receptor phytochrome B alter cell elongation and physiological responses throughout Arabidopsis development. *Plant Cell* **5**, 147-157.
Reed, J. W., Nagatani, A., Elich, T. D., Fagan, M. and Chory, J. (1994). Phytochrome A and phytochrome B have overlapping but distinct functions in Arabidopsis development. *Plant Physiol.* **104**, 1139-1149.
Ruegger, M., Dewey, E., Hobbie, L., Brown, D., Bernasconi, P., Turner, J., Muday, G. and Estelle, M. (1997). Reduced naphthylphthalamic acid binding in the tir3 mutant of Arabidopsis is associated with a reduction in polar auxin transport and diverse morphological defects. *Plant Cell* **9**, 745-757.
Sandhu, K. S., Hagely, K. and Neff, M. M. (2012). Genetic interactions between brassinosteroid-inactivating P450s and photomorphogenic photoreceptors in *Arabidopsis thaliana*. *G3* **2**, 1585-1593.
Savaldi-Goldstein, S., Peto, C. and Chory, J. (2007). The epidermis both drives and restricts plant shoot growth. *Nature* **446**, 199-202.
Schneider, C. A., Rasband, W. S. and Eliceiri, K. W. (2012). NIH Image to ImageJ: 25 years of image analysis. *Nat. Methods* **9**, 671-675.
Spartz, A. K., Lee, S. H., Wenger, J. P., Gonzalez, N., Itoh, H., Inzé, D., Peer, W. A., Murphy, A. S., Overvoorde, P. J. and Gray, W. M. (2012). The SAUR19 subfamily of *SMALL AUXIN UP RNA* genes promote cell expansion. *Plant J.* **70**, 978-990.
Symons, G. M., Ross, J. J., Jager, C. E. and Reid, J. B. (2008). Brassinosteroid transport. *J. Exp. Bot.* **59**, 17-24.
Szekeres, M., Németh, K., Koncz-Kálmán, Z., Mathur, J., Kauschmann, A., Altmann, T., Rédei, G. P., Nagy, F., Schell, J. and Koncz, C. (1996). Brassinosteroids rescue the deficiency of CYP90, a cytochrome P450, controlling cell elongation and de-etiolation in Arabidopsis. *Cell* **85**, 171-182.
Tanaka, K., Asami, T., Yoshida, S., Nakamura, Y., Matsuo, T. and Okamoto, S. (2005). Brassinosteroid homeostasis in Arabidopsis is ensured by feedback expressions of multiple genes involved in its metabolism. *Plant Physiol.* **138**, 1117-1125.
Tepperman, J. M., Hwang, Y.-S. and Quail, P. H. (2006). phyA dominates in transduction of red-light signals to rapidly responding genes at the initiation of Arabidopsis seedling de-etiolation. *Plant J.* **48**, 728-742.
Thornton, L. E., Rupasinghe, S. G., Peng, H., Schuler, M. A. and Neff, M. M. (2010). Arabidopsis CYP72C1 is an atypical cytochrome P450 that inactivates brassinosteroids. *Plant Mol. Biol.* **74**, 167-181.
Turk, E. M., Fujioka, S., Seto, H., Shimada, Y., Takatsuto, S., Yoshida, S., Denzel, M. A., Torres, Q. I. and Neff, M. M. (2003). CYP72B1 inactivates brassinosteroid hormones: an intersection between photomorphogenesis and plant steroid signal transduction. *Plant Physiol.* **133**, 1643-1653.
Turk, E. M., Fujioka, S., Seto, H., Shimada, Y., Takatsuto, S., Yoshida, S., Wang, H., Torres, Q. I., Ward, J. M., Murthy, G. et al. (2005). *BAS1* and *SOB7* act redundantly to modulate Arabidopsis photomorphogenesis via unique brassinosteroid inactivation mechanisms. *Plant J.* **42**, 23-34.
Vandenbussche, F., Verbelen, J.-P. and Van der Straeten, D. (2005). Of light and length: regulation of hypocotyl growth in Arabidopsis. *Bioessays* **27**, 275-284.
Vragović, K., Sela, A., Friedlander-Shani, L., Fridman, Y., Hacham, Y., Holland, N., Bartom, E., Mockler, T. C. and Savaldi-Goldstein, S. (2015). Translatome analyses capture of opposing tissue-specific brassinosteroid signals orchestrating root meristem differentiation. *Proc. Natl. Acad. Sci. USA* **112**, 923-928.
Wang, X. and Culver, J. N. (2012). DNA binding specificity of ATAF2, a NAC domain transcription factor targeted for degradation by Tobacco mosaic virus. *BMC Plant Biol.* **12**, 157.
Wang, Z.-Y. and Tobin, E. M. (1998). Constitutive expression of the *CIRCADIAN CLOCK ASSOCIATED 1* (*CCA1*) gene disrupts circadian rhythms and suppresses its own expression. *Cell* **93**, 1207-1217.
Wang, X., Goregaoker, S. P. and Culver, J. N. (2009). Interaction of the Tobacco mosaic virus replicase protein with a NAC domain transcription factor is associated with the suppression of systemic host defenses. *J. Virol.* **83**, 9720-9730.
Ward, J. M., Cufr, C. A., Denzel, M. A. and Neff, M. M. (2005). The Dof transcription factor OBP3 modulates phytochrome and cryptochrome signaling in Arabidopsis. *Plant Cell* **17**, 475-485.
Yokota, T. (1997). The structure, biosynthesis and function of brassinosteroids. *Trends Plant Sci.* **2**, 137-143.
Zhao, B. and Li, J. (2012). Regulation of brassinosteroid biosynthesis and inactivation F. *J. Integr. Plant Biol.* **54**, 746-759.
Zhao, J., Favero, D. S., Peng, H. and Neff, M. M. (2013). *Arabidopsis thaliana* AHL family modulates hypocotyl growth redundantly by interacting with each other via the PPC/DUF296 domain. *Proc. Natl. Acad. Sci. USA* **110**, E4688-E4697.
Zhao, J., Favero, D. S., Qiu, J., Roalson, E. H. and Neff, M. M. (2014). Insights into the evolution and diversification of the *AT-hook Motif Nuclear Localized* gene family in land plants. *BMC Plant Biol.* **14**, 266.
Zhu, J.-Y., Sae-Seaw, J. and Wang, Z.-Y. (2013). Brassinosteroid signalling. *Development* **140**, 1615-1620.

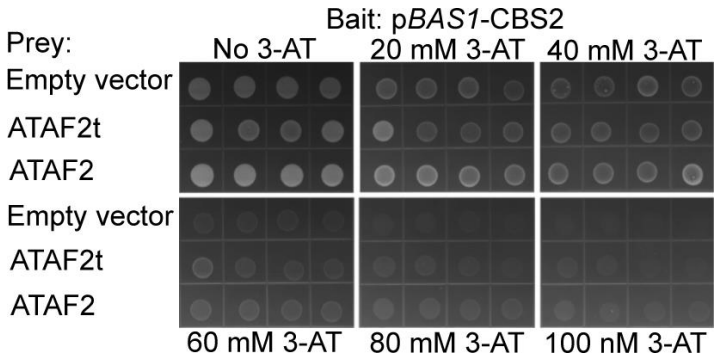

Fig. S1. Neither ATAF2t nor ATAF2 interacts with p*BAS1*-CBS2 in a targeted Y1H assay. Yeast integrated with p*BAS1*-CBS2 in the genome and transformed with the indicated prey plasmids were plated on selection medium supplemented with 3-AT of indicated concentrations (0, 20, 40, 60, 80 and 100 mM). Four independent clones were shown for each sample.

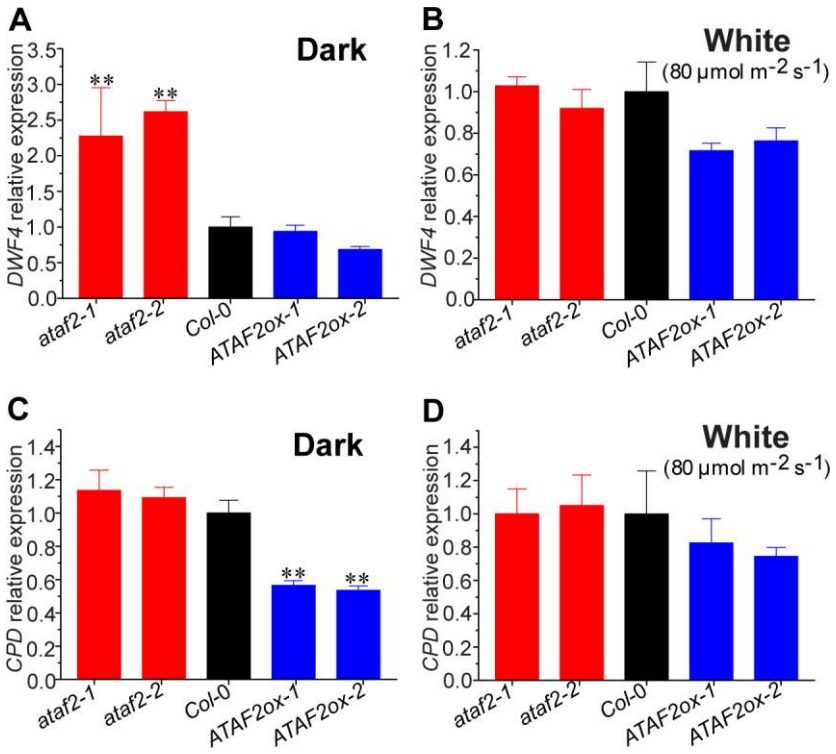

Fig. S2. Neither *DWF4* nor *CPD* is directly regulated by ATAF2. Neither *DWF4* (A,B) nor *CPD* (C,D) accumulation was dramatically changed in *ATAF2* loss- or gain-of-function seedlings. In darkness, the slight changes of *DWF* and *CPD* transcript accumulation in loss- and gain-of-function *ATAF2* mutants may be caused by the transcriptional feedback regulation due to altered BR levels. For each sample, around thirty four-day-old seedlings grown in 25 °C at the same time were grouped together and divided into three biological replicates before RNA extraction. Each qRT-PCR value is the mean of results from three biological replicates. Error bars denote the SEM. $*P < 0.05$, $**P < 0.01$, $***P < 0.001$ (unpaired one-tailed student's *t*-test). $n = 3$ for each value. *t*-tests were performed between the indicated sample group and the control group of *Col*-0.

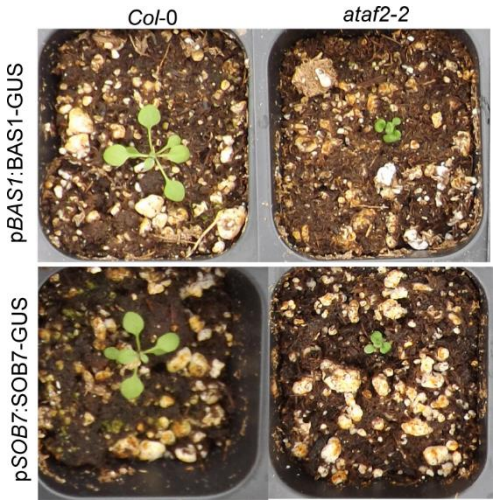

Fig. S3. T_1 primary transformants show BR-deficient dwarf phenotypes for both p*BAS1*:BAS1-GUS and p*SOB7*:SOB7-GUS transgenes. Ectopic expression of p*BAS1*:BAS1-GUS or p*SOB7*:SOB7-GUS could cause BR-deficient dwarfism in *ataf2-2*, but not in the wild-type plants (*Col*-0).

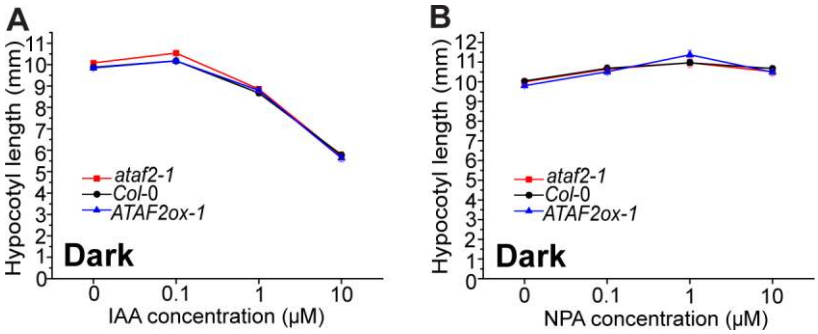

Fig. S4. Neither IAA (A) nor NPA (B) treatments affect the hypocotyl growth phenotypes of *ATAF2* loss- and gain-of-function seedlings in darkness. Treatments using either the auxin indole-3-acetic acid (IAA) or the auxin transport inhibitor naphthylphthalamic acid (NPA) did not significantly affect the hypocotyl growth phenotypes of *ATAF2* loss- and gain-of-function seedlings in darkness. This result suggests that auxins are not dominant players in ATAF2-mediated hypocotyl growth. Four-day-old seedlings grown in 25 °C were used for all the assays. Each sample value represents the average of measurement results from thirty seedlings. Error bars denote the SEM. n = 30 for each value. Unpaired two-tailed student's t-tests were performed between the indicated sample group and the control group of *Col*-0. No significant difference was detected.

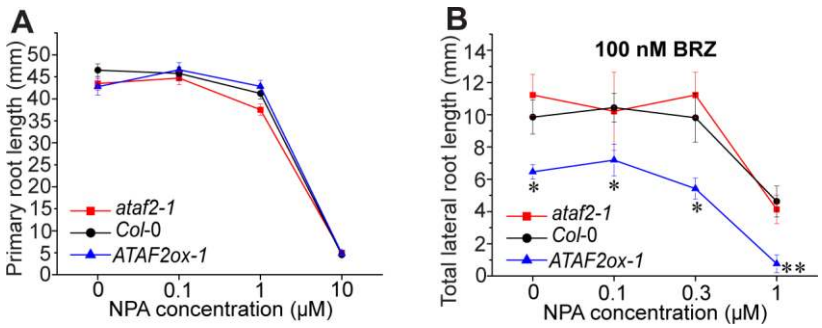

Fig. S5. Exogenous NPA treatments do not affect the root growth phenotypes of *ATAF2* loss- and gain-of-function seedlings. (A) Seven-day-old *ataf2-1* and *ATAF2ox* showed similar primary root growth in response to exogenous NPA treatments. (B) The lateral root growth phenotypes of ten-day-old *ataf2-1* and *ATAF2ox* seedlings under 100 nM BRZ were not affected by additional NPA treatments. Each sample value represents the average of measurement results from ten seedlings. Error bars denote the SEM. $*P < 0.05$, $**P < 0.01$, $***P < 0.001$ (unpaired two-tailed student's *t*-test). $n = 10$ for each value. *t*-tests were performed between the indicated sample group and the control group of *Col*-0.

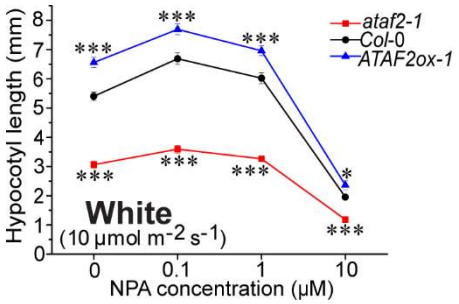

Fig. S6. Exogenous NPA treatments do not alter the hypocotyl growth phenotypes of *ATAF2* loss- and gain-of-function seedlings under low-fluence-rate (10 μmol m^{-2} s^{-1}) white light. Treatments using NPA did not affect the hypocotyl growth phenotypes of *ATAF2* loss- and gain-of-function seedlings, which suggests that auxins are not dominant players in ATAF2-mediated seedling photomorphogenesis. Four-day-old seedlings grown in 25 °C were used for the assay. Each sample value represents the average of measurement results from thirty seedlings. Error bars denote the SEM. *$P < 0.05$, **$P < 0.01$, ***$P < 0.001$ (unpaired two-tailed student's *t*-test). $n = 30$ for each value. *t*-tests were performed between the indicated sample group and the control group of *Col*-0.

Table S1. Sequences of *BAS1* and *SOB7* promoter fragments used for yeast-one-hybrid (Y1H) screen and targeted Y1H. The Evening Element (EE) and CCA1 binding site (CBS) are underlined.

Name	Sequence
p*BAS1*-EE	5'-CAGATTTTATCATATTATTTCTAAATGAGCGTTACGTTTTAAACTTTC AATTTTGTATATACACTATAGGTTTTGTGACAGGTCGATTATTATTGATA AAAGCATTGGGTTTACTGTATATTTTCTTTTTCTTTTTCAATTTCTTTTT TGCTAAAATGTTCATTTTTTCTTTTCTTATTTGATTCTGATATGCATGATT ATTTCAGGGAAAATATCTACATATCATAT-3'
p*BAS1*-CBS1	5'-AACCAATCGAATTATTCAAAAATCTTTATAATTAAATGACTGTTTTAA TACGCTAAACC-3'
p*BAS1*-CBS2	5'-ATAAATGTTAAGTTTAAACAATGACCTTAAAAATCTATATATAAGTT TTAAAAAACGTGTATTGA-3'
p*SOB7*-CBS	5'-AACAAATTTTTCCATTAATTCTACTAAGATTTTTAGGGTGTTGTTTT TGATGTTTTAAGTTTTTCTTATTTTTTGTCTTAATTTCTCCTCCTCCTATC TC-3'

Table S2. The short-hypocotyl phenotype of *ataf2-1* under low-fluence-rate (10 µmol m^{-2} s^{-1}) monochromatic red, far-red or blue light is attenuated when knocking out *PHYB* , *PHYA*, or *CRY1*, respectively. Unpaired two-tailed student's *t*-tests were performed between the indicated *photoreceptor ataf2-1* double mutant group and the control group of *ataf2-1* under the same light condition (10 µmol m^{-2} s^{-1} red, far-red, or blue light, respectively).

	Red (10 µmol m^{-2} s^{-1})	Far-red (10 µmol m^{-2} s^{-1})	Blue (10 µmol m^{-2} s^{-1})
	ataf2-1 hypocotyl length (%) against *Col-0* (average ± SEM):	*ataf2-1* hypocotyl length (%) against *Col-0* (average ± SEM):	*ataf2-1* hypocotyl length (%) against *Col-0* (average ± SEM):
	70.29 ± 2.07	**72.34 ± 1.33**	**71.00 ± 2.13**
	phyB-9 ataf2-1 hypocotyl length (%) against *phyB-9* (average ± SEM):	*phyA-211 ataf2-1* hypocotyl length (%) against *phyA-211* (average ± SEM):	*cry1-103 ataf2-1* hypocotyl length (%) against *cry1-103* (average ± SEM):
	79.01 ± 1.64	**96.45 ± 1.34**	**85.58 ± 2.02**
P	**0.00168**	**1.66E-18**	**4.58E-05**

Table S3. Primers used for quantitative RT-PCR (qRT-PCR).

Gene	Quantitative RT-PCR primers
UBQ10	5’-TCTTCGTGGTGGTTTCTAAATCTCG-3’
	5’-AAAGAGATAACAGGAACGGAAACATAGT-3’
ATAF2	5’-TTGGGTATCAAGAAAGCACTCGTC-3’
	5’-ACCCAATCATCAAGTCGTAGGTTG-3’
BAS1	5’- AATCCAGCTCGGTTTGCGGATG-3’
	5’-AGGCCAAACGGTATGAAGCCAAC-3’
SOB7	5’-GCTAAGCCACCTGAAAGTCGTAAC-3’
	5’-TCCGACATGTGAAGTAAGCTGGTG-3’
DWF4	5’-AATCCTTGGAGATGGCAACAGC-3’
	5’-TCTGAACCAGCACATAGCCTTGG-3’
CPD	5’- AGACCCAAACCACTTCAAAGATGC-3’
	5’- TGTCGTTACCGAGTTGCTCTGC-3’